iScience, Volume *23*

Supplemental Information

Hypothalamic and Cell-Specific Transcriptomes Unravel a Dynamic Neuropil Remodeling in Leptin-Induced and Typical Pubertal Transition in Female Mice

Xingfa Han, Laura L. Burger, David Garcia-Galiano, Seokmin Sim, Susan J. Allen, David P. Olson, Martin G. Myers Jr., and Carol F. Elias

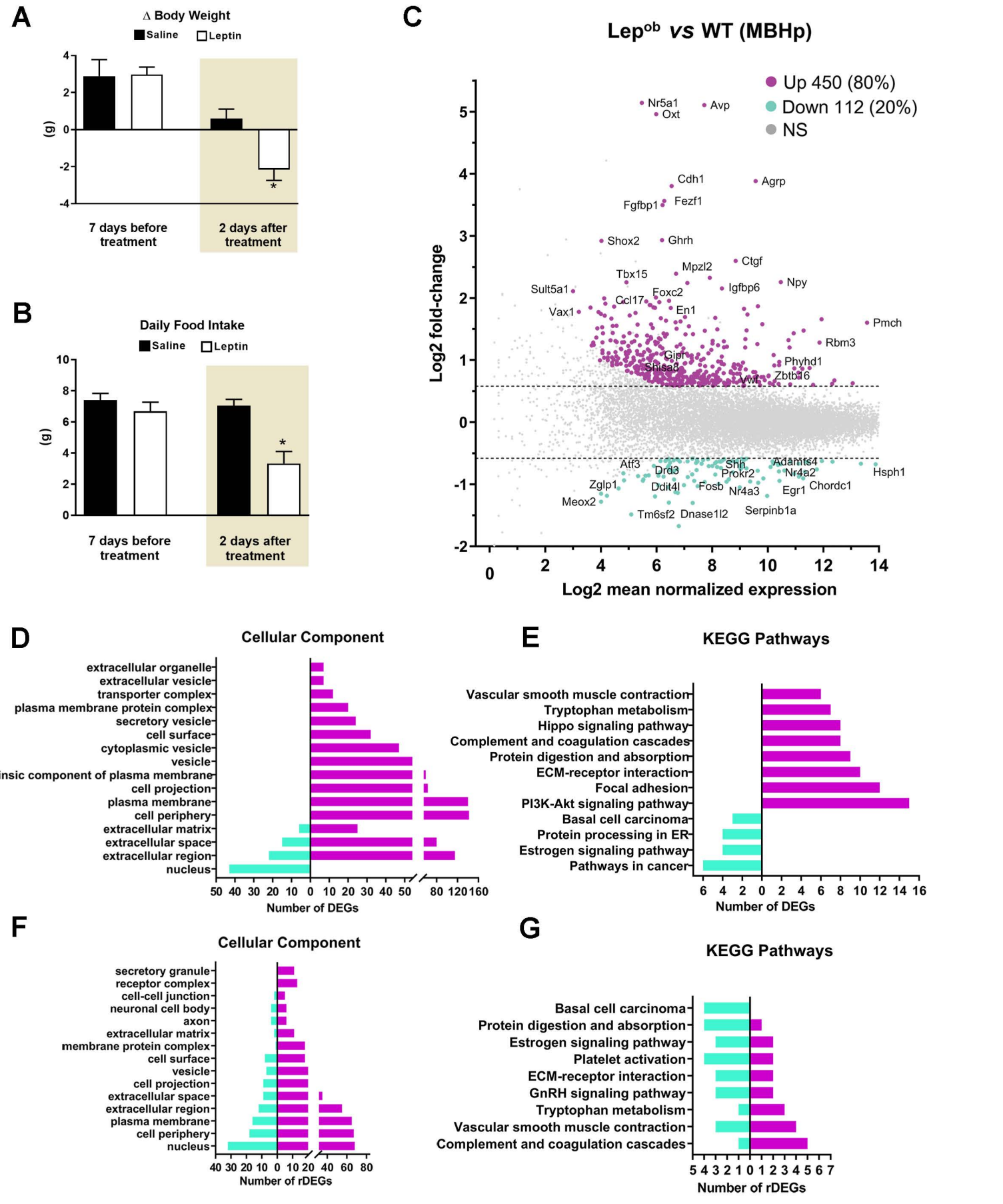

Figure S1. Related to Figure 1. (A-B) Changes in body weight and food intake of leptin-deficient Lep^{ob} mice before and after treatment with saline or leptin. Mice with clear vaginal opening were euthanized. (C) Differentially expressed genes (DEGs) in the posterior mediobasal hypothalamus (MBHp) between Lep^{ob} and WT female mice. GO (example of cellular compartment) and KEGG pathways of DEGs (D-E) and rDEGs (F-G) in the MBHp comparing Lep^{ob} vs WT (D-E) and Lep^{ob} vs Lep^{ob} + leptin (F-G). Purple, upregulated; Green, downregulated; NS, non significant.*p<0.05 by Student t test. Data presented as mean +/- SEM.

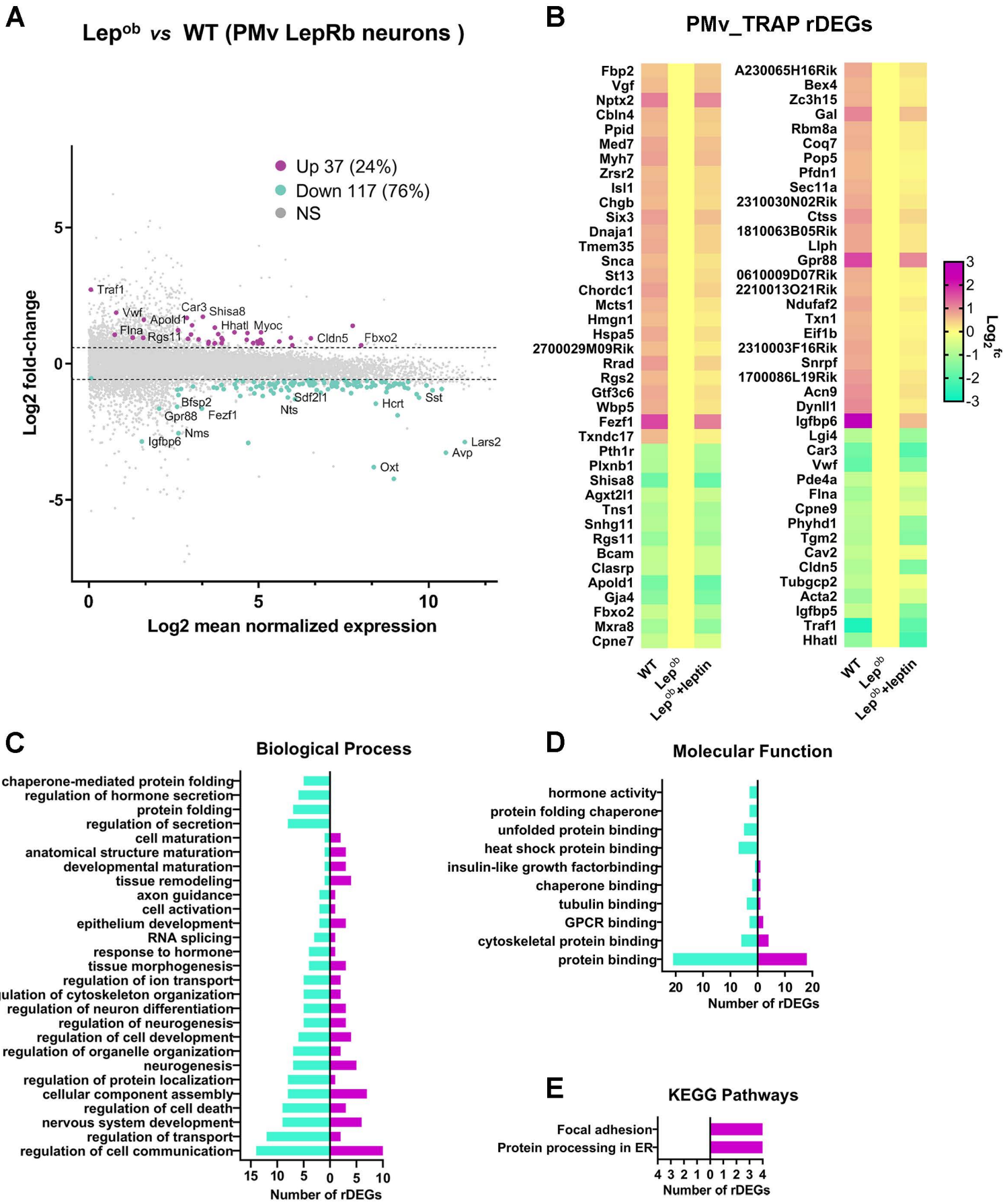

Figure S2. Related to Figure 2. Differentially expressed genes (TRAP_DEGs) in LepRb PMv neurons comparing Lep^{ob} and WT mice. (A) Most of the DEGs were downregulated in Lep^{ob} females. (B) recovered DEGs (rDEGs) enriched in PMv LepRb neurons. (C-E) GO and KEGG pathways associated with rDEGs. Purple, upregulated; Green, downregulated; NS, non-significant.

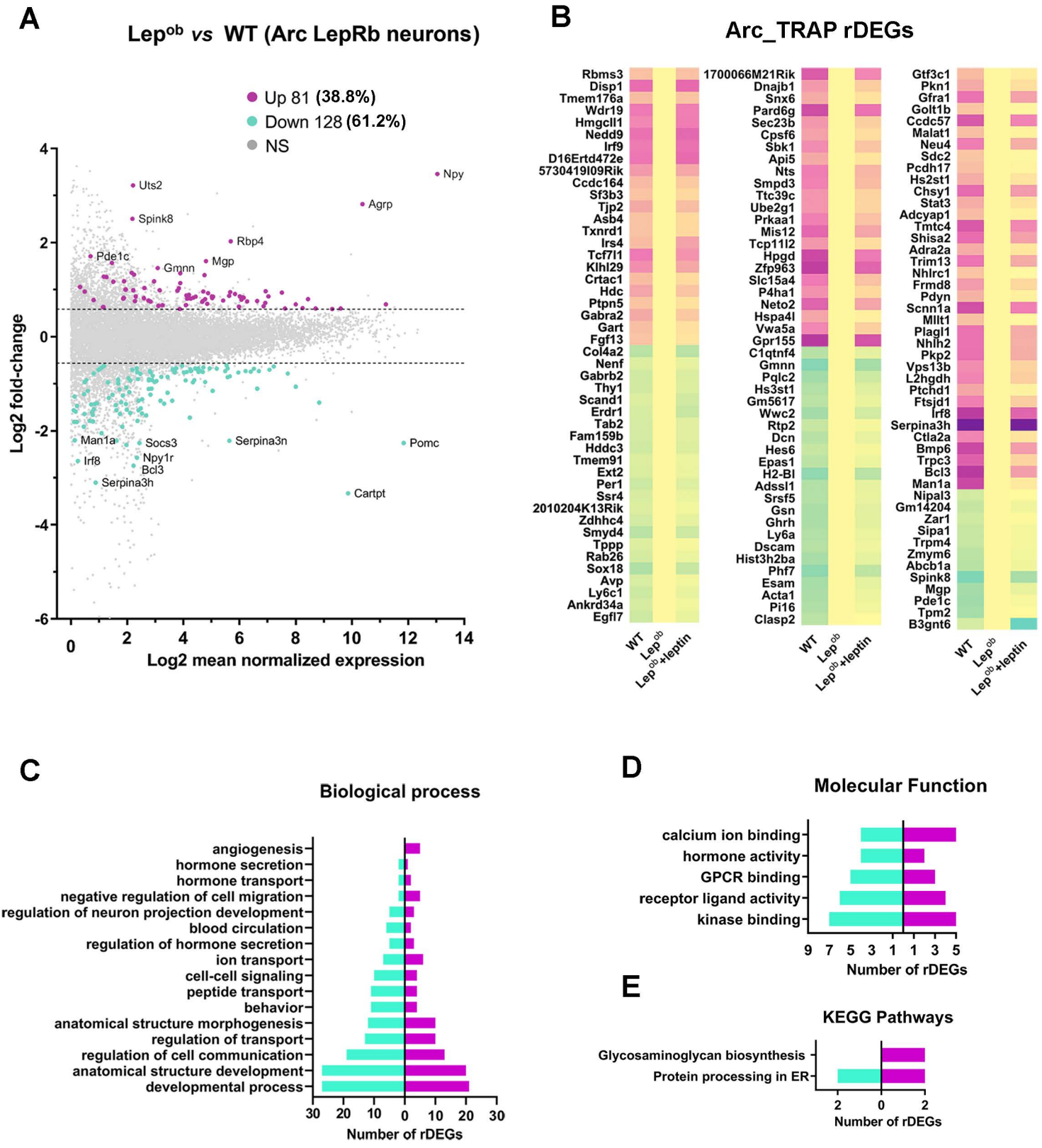

Figure S3. Related to Figure 2. Differentially expressed TRAP genes (TRAP_DEGs) in LepRb Arc neurons comparing Lep^{ob} and WT. (A) Most of these TRAP DEGs were downregulated in Lep^{ob} females. (B) recovered DEGs (rDEGs) after short-term leptin treatment. (C-E) GO and KEGG pathways associated with rDEGs. Purple, upregulated; Green, downregulated; NS, non significant.

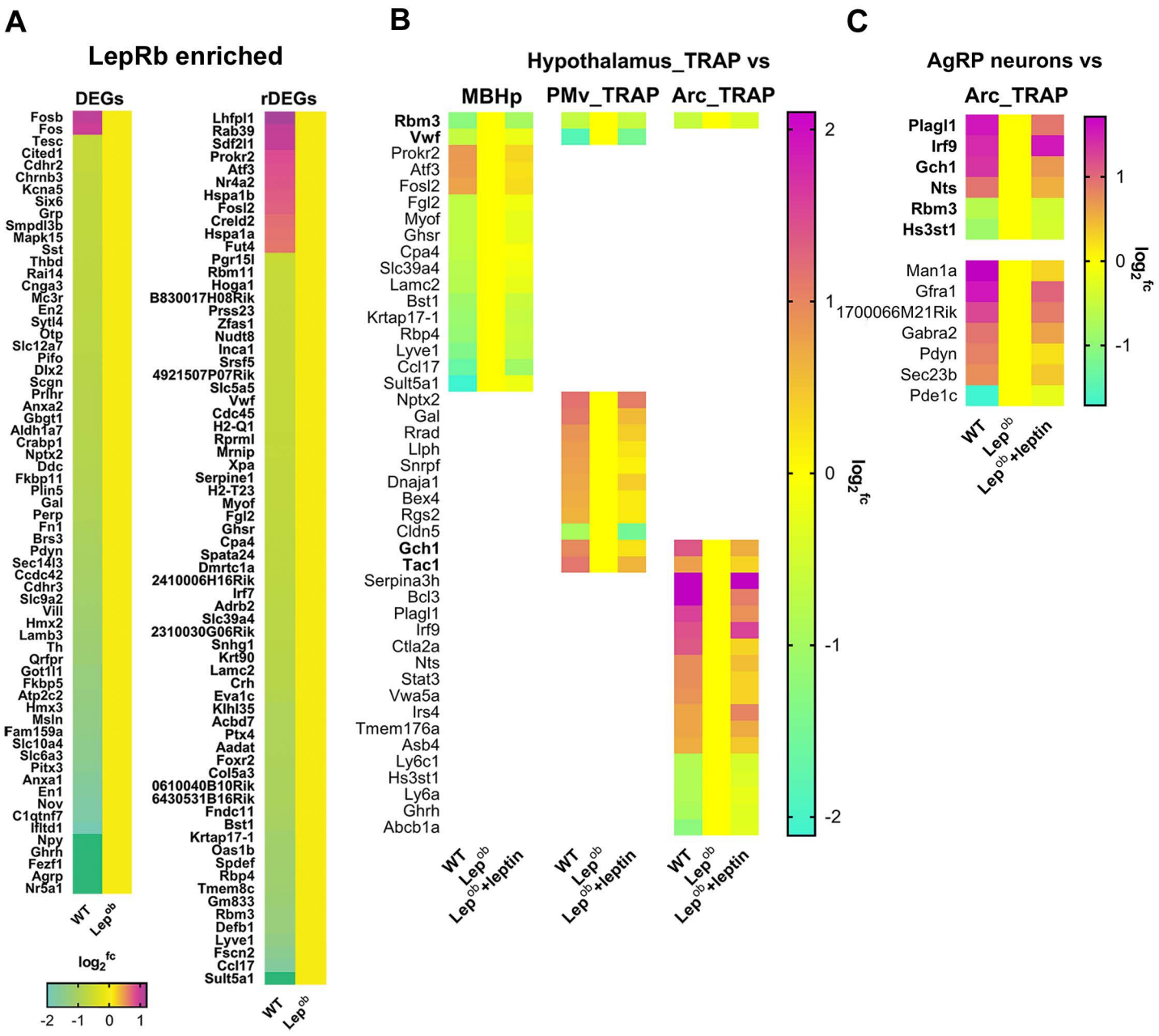

Figure S4. Related to Figure 2. Overlapping analysis using published database for further validation. A, B, comparative analysis of MBHp, PMv LepRb TRAP-seq, Arc LepRb TRAP-seq and TRAP DEGs obtained from hypothalamic blocks (Allison et al., 2015 and 2018). Only LepRb enriched and leptin regulated DEGs were used. C, Comparative analysis between Arc LepRb TRAP-seq and DEGs in AgRP neurons following nutritional challenges (Henry et al., 2015).

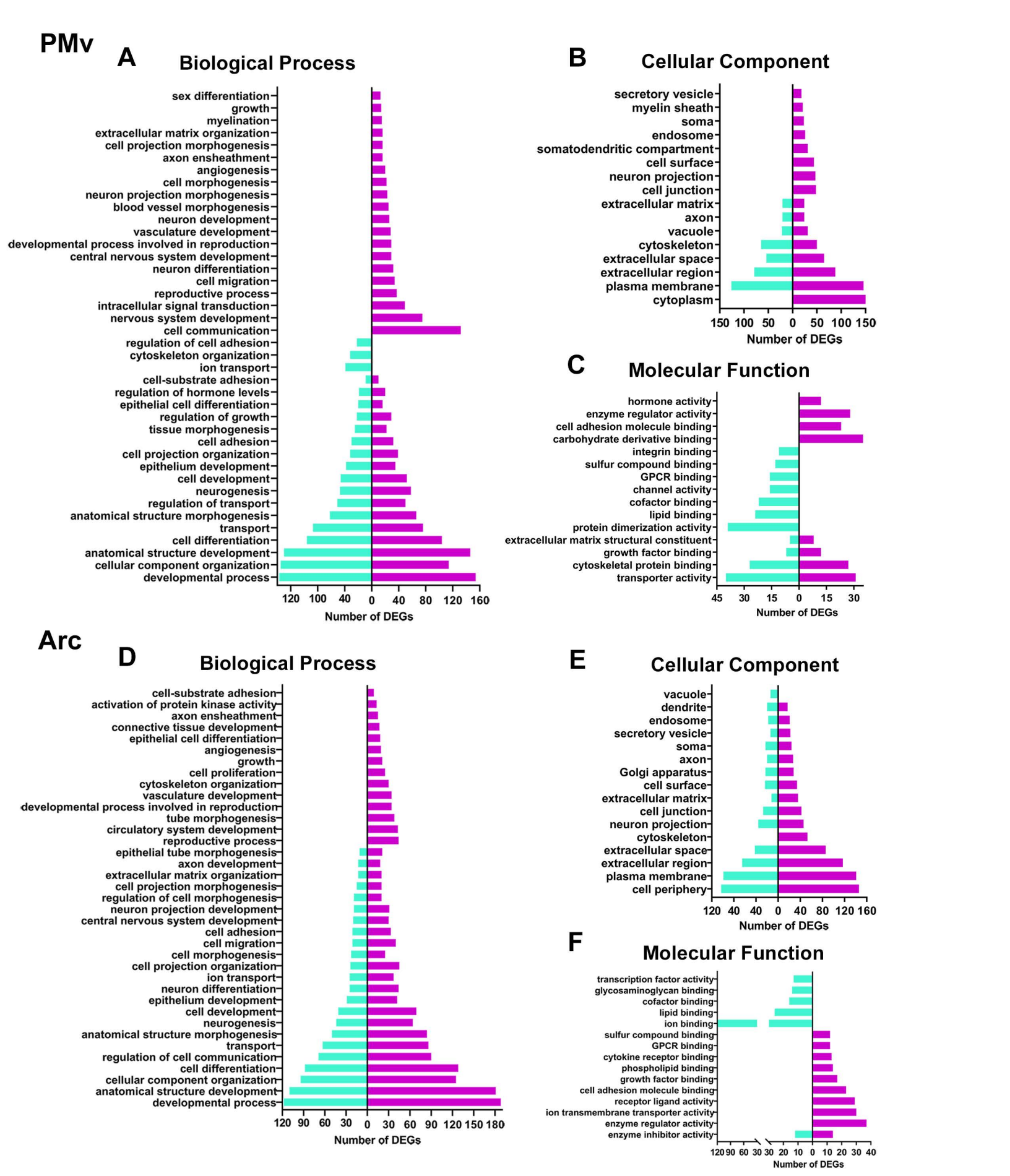

Figure S5. Related to Figure 3. Categorization of differentially expressed genes (DEGs) in the ventral premammillary nucleus (PMv, A-C) and arcuate nucleus (Arc, D-F) of prepubertal vs diestrous females.

Table S5: Primers used in qPCR.

Genes	Primer sequence (5'-3')	Product length (bp)
18s	F: TGACTCAACACGGGAAACC R: AACCAGACAAATCGCTCCAC	125
Ccl17	F: GCTGGTATAAGACCTCAGTGGAGTGT R: CAATCTGATGGCCTTCTTCACA	116
Cd46	F: ATGCCTGTGAACTACCACGGCCATTTGAAG R: TTTGCCAAATGAAGGGTCTTG	230
Crh	F: TCTGCAGAGGCAGCAGTGCGGG R: CGGATCCCCTGCTGAGCAGGGC	150
Gipr	F: CTGCCTGCCGCACGGCCCAGAT R: GCGAGCCAGCCTCAGCCGGTAA	383
Lhx9	F: CGTCTCTACGCTTCTGCATC R: GGCGGAAAGGACACGAAT	135
Meox2	F: TGGCAGCAAAAGGAAAAGCG R: GGAACCACACTTTCACCTGTCT	218
Nanos2	F: ATTCAGAGCCGGAAGCAAAG R: GACTGCTGTTGAGTGGACAA	285
Nr4a2	F: TTCCACCAGAACTACGTGGC R: CAGCTAGACACAGGAGTGCC	116
Pdlim3	F: TTGACAGGGCAGAAACTCGC R: GAAGCGCTCACTACCTGTCT	187
Pla2g3	F: GGGAACTCTGCTGAAAATGC R: AATGGTTTGTGGGCACTGAT	90
Rbp4	F: GACAAGGCTCGTTTCTCTGG R: AAAGGAGGCTACACCCCAGT	243
Shh	F: AGCAGACCGGCTGATGACTC R: TCACTCCAGGCCACTGGTTC	83
Shox2	F: TGGAACAACTCAACGAGCTGGAGA R: TTCAAACTGGCTAGCGGCTCCTAT	200
Wnt7a	F: GGCTACAACACACACCAGTAT R: GATCTGACCTGTGACCTCATTC	137
Zbtb16	F: CCTGGACAGTTTGCGACTGA R: TCCGTGCCAGTATGGGTCT	138
Zglp1	F: GGTTCAAGGGGGTAACTCTGG R: AGCAACTGGAACAACGGGTG	282

Note: F, Forward primer; R, Reverse primer

Transparent Methods

Key Resources Table

REAGENT or RESOURCE	SOURCE	IDENTIFIER
Antibodies		
Sheep anti-VWF antibody	Abcam Cat#ab11713	RRID:AB_298501
Rabbit anti-Laminin antibody	Novus Cat#NB300-144	RRID:AB_10001146
Rabbit anti-CART antibody	Phoenix Cat#H-003-62	RRID:AB_2313614
Goat anti-Rabbit IgG (H+L) Highly Cross-Adsorbed Secondary Antibody, Alexa Fluor Plus 488	Invitrogen Cat#A32731	RRID:AB_2633280
Donkey anti-Rabbit IgG (H+L) Highly Cross-Adsorbed Secondary Antibody, Alexa Fluor Plus 488	Invitrogen Cat#A32790	RRID:AB_2762833
Donkey anti-Sheep IgG (H+L) Cross-Adsorbed Secondary Antibody, Alexa Fluor 594	Invitrogen Cat#A-11016	RRID:AB_2534083
Chemicals, Peptides, and Recombinant Proteins		
Biotin-Protein L	GeneScript	Cat#M00097
BSA	Jackson Immuno Research	Cat#0001-000-162
Cycloheximide (CHX)	Sigma	Cat#C7698
Dithiothreitol Molecular Biology Reagent	Sigma	Cat#D9779
D-(+)-Glucose Bioxtra	Sigma	Cat#G7528
DHPC	Avanti Polar Lipids/VWR	Cat#100122-252
EDTA Free, Protease Cocktail Tablets	Roche	Cat#11836170001
GFP Ab, C8	Memorial-Sloan Kettering Monoclonal Antibody Facility	Cat#HTZ-GFP-19C8
GFP Ab, F7	Memorial-Sloan Kettering Monoclonal Antibody Facility	Cat#HTZ-GFP-19F7
HBSS, Hank'S balanced salt solution, 10X	Invitrogen/Life Technologies	Cat#14065-056
HEPES,1M	Affymetrix/Fisher	Cat#16924
iTaq™ Universal SYBR® Green Supermix	BIO-RAD	Cat#1725120
KCl, 2M	Applied Biosystems/Life Technologies	Cat#AM9640G
Leptin	A.F. Parlow, NHPP, Harbor-UCLA Medical Center, Torrance, California, USA	N/A
Methanol, Anhydrous, 99.8%	Sigma	Cat#322415
MgCl2, 1M	Applied Biosystems/Life Tech	Cat#AM9530G

NP-40, 10% Sterile, Rnase Free Vials	AG Scientific	Cat#P1505
PBS, 10X	Applied Biosystems/Life Tech	Cat#AM9625
QIAzol Lysis Reagent	Qiagen	Cat#79306
RNAsin	Promega/Fisher	Cat#N2515
RNAse Free Water	Applied Biosystems/Life Tech	Cat#AM9937
Roche Protector Rnase Inhibitor	Roche/Sigma	Cat#3335402001
Sodium Azide, 99.5%	Sigma	Cat#S2002
Sodium Bicarbonate Bioxtra	Sigma	Cat#S6297
Steptavidin T1 Dynabeads	Invitrogen/Life Technologies	Cat#65601
Superasin	Applied Biosystems/Life Tech	Cat#AM2694
Critical Commercial Assays		
DNAse I	Sigma-Aldrich	Cat#AMPD1
miRNeasy®mini Kit	Qiagen	Cat# 217004
Illumina TruSeq mRNA Sample Preparation v2 kit	Illumina	Catalog #s RS-122-2001, RS-122-2002
KAPA Library Quantification Kits	Kapa Biosystems	Cat# KK4835
RNeasy Micro Kit	Qiagen	Cat#74004
SMARTer Ultra Low RNA Kit for Illumina Sequencing	Clontech	Cat#634936
SuperScript™ II	Invitrogen	Cat#18064022
Deposited Data		
Sequencing data listed in the Tables	This paper	Table S1-4
Experimental Models: Organisms/Strains		
C57BL/6J mice	Jackson labs	Stock # 000664
$Lep^{ob/+}$ mice	Jackson labs	Stock # 000632
$LepR^{cre}$ mice	Leshan et al., 2006	N/A
$Rosa^{eGFP\text{-}L10a/eGFP\text{-}L10a}$ mice	Krashes et al., 2014	N/A
Oligonucleotides		
Primers for qPCR quantification	This paper	See Table S5
Software and Algorithms		
CiiiDER	Gearing et al., 2019	http://ciiider.com/
Cytoscape(v3.7.2)	Cytoscape Software	http://www.cytoscape.org/
Cufflinks/Cuffdiff(2.1.1)	Trapnell et al., 2012	http://cole-trapnell-lab.github.io/cufflinks/install/
DAVID(v6.8)	Huang da et al., 2009	https://david.ncifcrf.gov/
GraphPad Prism (v8.0)	GraphPad Software	https://www.graphpad.com/

R (v 3.6.1)	R Software	https://www.R-project.org/
STRING (v11.0)	String Consortium	https://string-db.org/cgi/input.pl
TopHat (v2.0.13)	Trapnell et al., 2012	http://ccb.jhu.edu/software/tophat/downloads/
VLAD (v1.8.0)	Richardson & Bult, 2015	http://proto.informatics.jax.org/prototypes/vlad/

Experimental Model and Subject Details

Mice

$Lep^{ob/+}$ mouse (ob/+; JAX® mice, stock # 000632) purchased from Jackson labs were intercrossed to generate $Lep^{+/+}$ (WT) and $Lep^{ob/ob}$ (Lep^{ob}) female littermates. $Lep^{ob/+}$ mice were crossed to $LepR^{cre}$ (Leshan et al., 2006) to obtain $Lep^{ob/+}LepR^{cre}$ mice, which were subsequently crossed to $Rosa^{eGFP\text{-}L10a/eGFP\text{-}L10a}$ mice (Allison et al., 2015; Krashes et al., 2014) to generate $Lep^{ob/+}LepRb^{cre}Rosa^{eGFP\text{-}L10a}$ (LepRbLepR$^{eGFP\text{-}L10a}$) mice, which express GFP-labeled L10a ribosomal protein targeted to LepRb neurons. $Lep^{ob/+}LepRb^{cre}Rosa^{eGFP\text{-}L10a}$ mice were then intercrossed to generate $Lep^{+/+}$; $LepRb^{cre/cre}Rosa^{eGFP\text{-}L10a/eGFP\text{-}L10a}$ and $Lep^{ob/ob}LepRb^{cre/cre}Rosa^{eGFP\text{-}L10a/eGFP\text{-}L10a}$ ($LepRb^{eGFP\text{-}L10a}$) female littermates. Adult (PND60-70) and prepubertal (PND18) C57BL/6J females were generated from the intercrossing of C57BL/6J mice (JAX® mice, stock # 000664). Mice were bred at the University of Michigan and maintained in a light- (12 h light/dark cycle) and temperature- (21 to 23°C) controlled environment with free access to water and food. Mice were fed with a phytoestrogen-reduced diet 2016 (16% protein/4% fat, Teklad 2916 irradiated global rodent diet, Envigo) to minimize the effect of exogenous estrogen in pubertal development. All procedures involving mice were approved by the University of Michigan IACUC in accordance with AAALAC and NIH guidelines (protocol # PRO08712).

Methods

Leptin treatment and harvesting of MBHp

Mice (PND60-70) were divided into three groups (n=4/group): a) wildtype (WT) diestrous females treated with intraperitoneal (ip.) saline; b) leptin-deficient (Lep^{ob}) females treated with ip. saline (ob); and c) Lep^{ob} females treated with ip. leptin (Lep^{ob}+leptin) 2.5 μg/g for 2 days, at 9:00 AM and 5:00 PM (leptin from A.F. Parlow, Harbor-UCLA Medical Center, National Hormone and Peptide Program). One hour after the last saline or leptin injection (at 10:00 AM), females were euthanized by decapitation following anesthesia (isoflurane) and brains were harvested. Frontal sections of the hypothalamus (1 mm-thick) were collected using a brain matrix (Ted Pella, Inc. cat# 15003). The MBHp was micro-dissected, processed for RNA extraction and submitted for RNAseq analysis.

Translating Ribosome Affinity Purification (TRAP) of PMv and Arc LepRb cells

Diestrous $LepR^{eGFP\text{-}L10a}$ and $Lep^{ob}LepR^{eGFP\text{-}L10a}$ female mice (PND60-70) were used. The expression of eGFP-L10a in LepRb neurons in the hypothalamus of the $LepR^{eGFP\text{-}L10a}$ mouse line has been verified and validated by our group (Allison et al., 2018; Allison et al., 2015).The experimental design and saline/leptin treatment were the same as detailed in the previous item ("Leptin treatment and harvesting of MBHp"). The PMv and Arc were collected separately from the left and right sides of each individual mouse brain by micro punches (1.25 mm diameter). The third ventricle was used as anatomical reference for the medial and dorsal borders of the hypothalamus and the fornix was used as the lateral limit of the medial hypothalamus. Preliminary experiments assessing RNA concentration determined the need to pool micro punches from both sides of three mice per treatment group. Each pooled set of PMv or Arc punches was considered a single biological replicate, and four biological replicates in each treatment group were used. The mRNA was isolated from eGFP-tagged ribosomes, as well as eGFP-depleted supernatant (Allison et al., 2015; Burger et al., 2018; Heiman et al., 2014). Tissue punches were immediately homogenized in ice-cold lysis buffer [20 mM HEPES-KOH, 150 mM KCl, and 10 mM $MgCl_2$ (Affymetrix/Thermo Fisher Scientific); 1× EDTA Free Protease Inhibitor and 1.25% volume-to-volume ratio (v/v) of RNAse Inhibitor (Roche, Indianapolis, IN), 0.625% v/v RNAsin (Promega, Madison, WI), 0.625% v/v Superasin (Invitrogen/Thermo Fisher Scientific), 0.5 mM dithiothreitol and 0.1 mg/ml cycloheximide. Lysis buffer volume was adjusted for input amounts of PMv and Arc punches (100 µL of lysis buffer per punches). Anti-GFP (HtzGFP-19F7 and HtzGFP-19C8; Antibody and Bioresource Core Facility, Memorial Sloan Kettering Cancer Center, New York, NY)-coated streptavidin magnetic beads (Streptavidin T1 Dynabeads; Invitrogen/Thermo Fisher Scientific) were applied to the samples. Immunoprecipitation occurred overnight at 4°C. Polysome-RNA complexes bound to the anti–GFP-coated streptavidin magnetic beads (LepRb neuron specific) were separated from the supernatant by a magnet; RNA was isolated using the RNeasy Micro Kit with on-column DNAsin (Qiagen, Valencia, CA). The RNA samples were subjected to RNA quantification and quality evaluation using the RNA 6000 Pico Chip (Agilent Technologies) for RNAseq. Before generating cDNA libraries, LepRb-enhanced and LepRb-depleted RNAs were reverse transcribed (Allison et al., 2018; Allison et al., 2015; Burger et al., 2018) and amplified for *Lepr* and *Actb* (β-actin, reference gene) using Taqman qPCR to determine enrichment for *Lepr*. The *Lepr* expression levels were normalized to *Actb* (no difference between groups), and enrichment was calculated as relative expression in LepRb-enhanced RNA samples divided by the normalized relative expression in the LepRb-depleted samples. The LepRb-enhanced RNA of each sample was used to create cDNA libraries with the SMARTer v4 Ultra Low Kit and Low Input DNA library Pre Kits (Clontech) (Burger et al., 2018).

Tissue harvesting in prepubertal vs diestrus females

C57BL/6J prepubertal (P18) and adult diestrous (P60-70) females (n=4 per group) were euthanized under isoflurane anesthesia. Vaginal cytology was monitored for approximately 7 days before tissue collection in adult females to determine estrous cycle stage. Only normally cycling females were used. After euthanasia, uterine weight was measured to confirm diestrus (< 100 mg). PMv and Arc micro punches were dissected and collected as detailed in the

previous section (“Translating Ribosome Affinity Purification (TRAP) of PMv and Arc LepRb cells”) and processed for RNAseq analysis.

RNA-sequencing and Data Processing

RNA was extracted with miRNeasy®mini Kit (Qiagen, cat# 217004) according to the manufacturer protocol. RNA was assessed for quality using the TapeStation (Agilent, Santa Clara, CA). Samples with RNA integrity numbers (RINs) of 8 or greater were subjected to Illumina TruSeq mRNA Sample Preparation v2 kit (Catalog #s RS-122-2001, RS-122-2002), and 1-3g of total RNA was purified to mRNA using polyA purification. The mRNA was fragmented via chemical fragmentation and reverse transcribed into cDNA using reverse transcriptase and random primers. The 3’ ends of the cDNA were adenylated, and 6-nucleotide-barcoded adapters ligated. The products were purified and enriched by PCR to generate the final cDNA library. Final libraries were checked for quality and quantity by TapeStation (Agilent) and qPCR using Kapa's library quantification kit for Illumina Sequencing platforms (Kapa Biosystems, cat# KK4835). They were clustered on the cBot (Illumina) and 4 samples per lane were sequenced on a 50-cycle single end run in a HiSeq 2500 (Illumina) by the University of Michigan DNA Sequencing and Bioinformatics Cores. The Tuxedo Suite software package was used for alignment, differential expression analysis, and post-analysis diagnostics (Trapnell et al., 2013). Cufflinks/CuffDiff (http://coletrapnell-lab.github.io/cufflinks/) (Trapnell et al., 2012) was used for quantitation, normalization, and determination of differential expression using University of California Santa Cruz (Santa Cruz, CA) mm10.fa as the reference genome sequence (http:// genome.ucsc.edu/). Hierarchical cluster analysis was conducted to assemble genes with similar expression patterns across groups using Cluster 3.0 software. After normalization of the expression of each gene by log2 transformation, gene clustering was performed with average linkage method with Euclidean distance. The hierarchical cluster heatmap was organized by Java TreeView software. DEGs in pairwise comparisons among groups were determined using Cufflinks/Cuffdiff analysis, with thresholds for differential expression set to fold change (fc)>1.5 or <0.66 and a false discovery rate (q value) of ≤ 0.05. The Gene List analysis and Visualization (VLAD) v1.8.0 was used to define the enriched biological processes (BP), cellular component (CC) and molecular function (MF) of DEGs. For pathway analysis, the Kyoto Encyclopedia of Genes and Genomes (KEGG) pathway database using DAVID v6.8 was used to reveal physical and/or functional interactions among the genes. Gene ontology (GO) and pathway terms showing unadjusted p-values < 0.05 were selected. STRING online database (http://string-db.org) was used to assess protein-protein interaction (PPI) and Cytoscape software (http://www.cytoscape.org/) was employed to visualize PPI network interaction of common DEGs.

Mapping of phosphoSTAT binding sites

The potential pSTAT3/STAT5 binding sites across the promoter region (1500bp upstream and 500bp downstream of the transcription start site) of the core genes were scanned by CiiiDER software. JASPAR2020_CORE_vertebrates clustering was used as the transcription factor position frequency matrix. Deficit threshold was defined as 0.15. One thousand genes with close to zero-fold change between WT and Lep^{ob} from PMv TRAP-seq and Arc TRAP-seq, respectively, were used as the background gene list to identify significantly over-represented

STAT3/STAT5-targeting core genes in PMv and Arc, respectively. Fisher's exact test was used and gene coverage p-value < 0.05 was considered significant.

Analysis of Overlapping DEGs in all three RNAseq Assays

All analyses were generated in R (v3.6.1) language for statistical computing (https://www.R-project.org/). Independent RNA-seq data (MBHp, TRAPseq, and PP vs Di CuffDiff results) and DAVID enrichments were used as input files (Huang da et al., 2009a, b; Trapnell et al., 2012). To determine shared DAVID functional enrichments between comparisons from different projects, shared DEGs and identity of all measured genes across the comparisons were first determined. Group comparisons:

Group 1: WT_v_Ob_Saline_DE.xlsx (MBHp), PMV.diestrus_v_PMV.ob_saline.xlsx (TRAPseq), PMV.Adult_v_PMV.Pre.xlsx (PP vs Di);

Group 2: WT_v_Ob_Saline_DE.xlsx (MBHp), ARC.diestrus_v_ARC.ob_saline.xlsx (TRAPseq), ARC.Adult_v_ARC.Pre.xlsx (PP vs Di);

Group 3: Supp Table 1 DEGs (MBHp), Supp Table 4 PMV DEGs (TRAPseq), PMV.Adult_v_PMV.Pre.xlsx (PP vs Di);

Group 4: Supp Table 1 DEGs (MBHp), Supp Table 6 Arc DEGs (TRAPseq), ARC.Adult_v_ARC.Pre.xlsx (PP vs Di)

Shared DEGs and all measured genes between comparison sets were converted from gene symbols to ENSEMBL ids and used as query sets and background sets, respectively, for DAVID enrichments using R package RDAVIDWebService (v3.10) (Fresno and Fernandez, 2013). Enrichments were repeated with rDEGs as query sets for Group 3 and Group 4. The background sets generated for Group 1 (PMv) and Group 2 (Arc) were used for DEGs and rDEG DAVID enrichments for Group 3 (PMv) and Group 4 (Arc), matched by cell-type.

Quantitative PCR (qPCR) validation of RNA-sequencing data

To validate the RNAseq data, PMv and Arc samples obtained by micro punches were evaluated. Tissue was homogenized in Qiazol reagent (Qiagen), and total RNA was isolated using an RNA extraction kit (miRNeasy, Qiagen). Total RNA (200 ng) was used to synthesize cDNA using SuperScript II reverse transcriptase and random primers (Invitrogen) according to the manufacturer's protocol. Gene expression analyses were performed by qPCR using a CFX-384 Bio-Rad Real-Time PCR detection system (SYBR Green reaction).The mRNA levels were normalized to the *18s* ribosomal RNA reference gene, and changes related to the control levels (WT, diestrous females) were determined using $2^{-\Delta\Delta Ct}$ method. We initially evaluated the variation of *18s* Ct values across samples and experiment groups and no difference was observed (all groups showed Ct values ranging from 12.8 to 13.4) indicating the *18s* was an adequate reference gene. Primers for targeted and reference genes are listed in Table S5.

Immunofluorescence

A group of PP and Di mice were intracardially perfused with 10% formalin, and brains were prepared for histological examination. Hypothalamic sections of PP and Di females were labeled with sheep anti-VWF (1:1,000 Abcam, cat#ab11713) and/or rabbit anti-Laminin (1:1000 Novus, cat#NB300-144). According to the manufacturers, the laminin antibody is pan-specific and

reacts with all laminin isoforms tested: Laminin-1 (alpha-1, beta-1, and gamma-1) and Laminin-2 (alpha-2, beta-1, and gamma-1). Following overnight incubation at room temperature, tissue was incubated in secondary conjugated to AF488 or AF594 (Invitrogen) for 1h. Another series of hypothalamic sections from PP and Di mice were also incubated in rabbit anti-CART peptide (1:10,000 Phoenix, cat#H-003-62) and processed for immunoperoxidase using DAB and silver enhancement.

QUANTIFICATION AND STATISTICAL ANALYSIS

Data other than RNAseq are reported as mean ± standard error of the mean (SEM) and were analyzed using the GraphPad Prism 7 software. Statistical analyses of RT-qPCR data and changes in body weight and food intake of Lep^{ob} mice before and after saline or leptin treatment were done by one-way ANOVA followed by Tukey's test. Quantification of CART-ir fiber density was performed in one section and one side of the Arc (n=3/group) at the tuberal level (image 67, Allen Mouse Brain Atlas). Fiber density was quantified by integrated optical density using fixed illumination, background normalization and gray scale in Image J (NIH). Quantification of colocalization between GFP- and Laminin-ir was performed in one section and one side of the PMv (n=4-5, Image 76, Allen Mouse Brain Atlas). F test to compare variances and one-way ANOVA followed by Tukey's test were used. Significance was set at $p< 0.05$.

References

Allison, M.B., Pan, W., MacKenzie, A., Patterson, C., Shah, K., Barnes, T., Cheng, W., Rupp, A., Olson, D.P., and Myers, M.G., Jr. (2018). Defining the Transcriptional Targets of Leptin Reveals a Role for Atf3 in Leptin Action. Diabetes *67*, 1093-1104.

Allison, M.B., Patterson, C.M., Krashes, M.J., Lowell, B.B., Myers, M.G., Jr., and Olson, D.P. (2015). TRAP-seq defines markers for novel populations of hypothalamic and brainstem LepRb neurons. Mol Metab *4*, 299-309.

Burger, L.L., Vanacker, C., Phumsatitpong, C., Wagenmaker, E.R., Wang, L., Olson, D.P., and Moenter, S.M. (2018). Identification of Genes Enriched in GnRH Neurons by Translating Ribosome Affinity Purification and RNAseq in Mice. Endocrinology *159*, 1922-1940.

Fresno, C., and Fernandez, E.A. (2013). RDAVIDWebService: a versatile R interface to DAVID. Bioinformatics *29*, 2810-2811.

Heiman, M., Kulicke, R., Fenster, R.J., Greengard, P., and Heintz, N. (2014). Cell type–specific mRNA purification by translating ribosome affinity purification (TRAP). Nature Protocols *9*, 1282.

Huang da, W., Sherman, B.T., and Lempicki, R.A. (2009a). Bioinformatics enrichment tools: paths toward the comprehensive functional analysis of large gene lists. Nucleic Acids Res *37*, 1-13.

Huang da, W., Sherman, B.T., and Lempicki, R.A. (2009b). Systematic and integrative analysis of large gene lists using DAVID bioinformatics resources. Nat Protoc *4*, 44-57.

Krashes, M.J., Shah, B.P., Madara, J.C., Olson, D.P., Strochlic, D.E., Garfield, A.S., Vong, L., Pei, H., Watabe-Uchida, M., Uchida, N.*, et al.* (2014). An excitatory paraventricular nucleus to AgRP neuron circuit that drives hunger. Nature *507*, 238-242.

Leshan, R.L., Bjornholm, M., Munzberg, H., and Myers, M.G., Jr. (2006). Leptin receptor signaling and action in the central nervous system. Obesity (Silver Spring) *14 Suppl 5*, 208S-212S.

Trapnell, C., Hendrickson, D.G., Sauvageau, M., Goff, L., Rinn, J.L., and Pachter, L. (2013). Differential analysis of gene regulation at transcript resolution with RNA-seq. Nat Biotechnol *31*, 46-53.

Trapnell, C., Roberts, A., Goff, L., Pertea, G., Kim, D., Kelley, D.R., Pimentel, H., Salzberg, S.L., Rinn, J.L., and Pachter, L. (2012). Differential gene and transcript expression analysis of RNA-seq experiments with TopHat and Cufflinks. Nat Protoc *7*, 562-578.